ELSEVIER

Contents lists available at ScienceDirect

Carbohydrate Polymers

journal homepage: www.elsevier.com/locate/carbpol





Fucoidans inhibited tau interaction and cellular uptake

Weihua Jin ^{a,b}, Chenghui Lu ^a, Yanan Zhu ^c, Jing Zhao ^{b,d}, Wenjing Zhang ^e, Lianchun Wang ^c, Robert J. Linhardt ^{b,f}, Chunyu Wang ^{b,*}, Fuming Zhang ^{b,*}

- ^a College of Biotechnology and Bioengineering, Zhejiang University of Technology, Hangzhou 310014, China
- b Department of Chemical and Biological Engineering, Center for Biotechnology and Interdisciplinary Studies, Rensselaer Polytechnic Institute, Troy, NY 12180, USA
- ^c Department of Molecular Pharmacology and Physiology, Byrd Alzheimer's Research Institute, Morsani College of Medicine, University of South Florida, Tampa, USA
- ^d College of Food Science and Nutritional Engineering, China Agricultural University, Beijing 100083, China
- ^e Department of Endocrinology and Metabolism, Sir Run Run Shaw Hospital, Zhejiang University School of Medicine, Hangzhou 310016, China
- f Department of Biological Science, Departments of Chemistry and Chemical Biology and Biomedical Engineering, Center for Biotechnology and Interdisciplinary Studies, Rensselaer Polytechnic Institute, Troy, NY 12180, USA

ARTICLE INFO

Keywords: Alzheimer's disease Heparin Fucoidans Tau protein Sulfated glycan

ABSTRACT

Tau spreading in Alzheimer's disease is mediated by cell surface heparan sulfate (HS). As a class of sulfated polysaccharides, fucoidans might compete with HS to bind tau, resulting in the cessation of tau spreading. The structural determinants of fucoidans for competition with HS binding to tau are not well understood. Sixty previously prepared fucoidans/glycans with different structural determinants were used to determine their binding abilities to tau using SPR and AlphaLISA. Finally, it was found that fucoidans had two fractions (sulfated galactofucan (SJ-I) and sulfated heteropolysaccharide (SJ-GX-3)), which exhibited strong binding abilities than heparin. Tau cellular uptake assays using wild type mouse lung endothelial cell lines were performed. It was shown SJ-I and SJ-GX-3 inhibited tau-cell interaction and tau cellular uptake, suggesting that fucoidans might be good candidates for inhibiting tau spreading. NMR titration mapped fucoidans binding sites, which could provide the theoretical basis for the design of tau spreading inhibitors.

1. Introduction

Alzheimer's disease (AD), the most common cause of dementia in older adults, is an irreversible, progressive brain disorder that slowly destroys memory and thinking skills, eventually, the ability to do the simplest tasks (Aging, 2020; Scheltens et al., 2016). According to the 2020 Alzheimer's association report, the official death certificates recorded 122,019 deaths from AD in 2018, making AD as the sixth leading cause of death in the United States and the fifth leading cause of death of Americans, who are 65 and older (2020 Alzheimer's disease facts and figures, 2020). As the population of AD increases, the burden will also increase, leading to the urgency of finding a cure.

However, the pathological mechanism of AD was complex. Senile plaques formed by the amyloid β (A β) outside neurons in the brain and neurofibrillary tangles (NFTs) formed by hyperphosphorylated tau or aggregated tau inside neurons are the two major reasons associated with AD, accompanying with neuroinflammation, virus infection, metal ions deficiencies and other abnormalities (Cairns et al., 2020; Drago, Bolognin, & Zatta, 2008; Ising et al., 2019; Shi et al., 2020). There were

54 % of the AD drugs targeting $A\beta$ in phase III clinical trials, however, no drugs targeting $A\beta$ was successful, leading to reject the amyloid cascade hypothesis (Cummings, Lee, Ritter, & Zhong, 2018; Doig et al., 2017; Herrup, 2015). Doig et al. (2017) proposed that drugs should be targeting tau pathology, rather than $A\beta$, which was identified in the other researches (Giacobini & Gold, 2013; Roberson et al., 2007).

Tau, expressed predominantly in the central and peripheral nervous systems, can be divided into an N-terminal projection domain, a prolinerich region, a repeat region, and a C-terminal domain (Goedert, Eisenberg, & Crowther, 2017). Tau is also a major regulator of microtubules (MTs) formation in cells (Lindwall & Cole, 1984; Weingarten, Lockwood, Hwo, & Kirschner, 1975). There are many causes, including an imbalance of tau kinases and/or phosphatases, mutations of the tau gene, covalent modification of tau causing and/or promoting tau misfolding and others, resulting in the detachment of tau from the MTs (Ballatore, Lee, & Trojanowski, 2007; Lindwall & Cole, 1984). Once tau unbinds from the MTs, a cascaded reaction is initiated. At first, tau becomes more likely to misfold, followed by deposits (also called pretangles) and β -sheet (containing paired helical filament), and NFTs are

E-mail addresses: wangc5@rpi.edu (C. Wang), zhangf2@rpi.edu (F. Zhang).

^{*} Corresponding authors.

finally formed. The level of NFTs was related to a demential degree (Shi et al., 2020). In addition, tau, unlike $A\beta$, spread through neural networks in a prion-like manner, driving the progression of neuronal degeneration (Brettschneider, Del Tredici, Lee, & Trojanowski, 2015; Chu & Liu, 2019; Goedert, Masuda-Suzukake, & Falcon, 2017; Holmes et al., 2014; Zhao et al., 2020). There were many ways mediated the transcellular movement of tau (Colin et al., 2020; Demaegd, Schymkowitz, & Rousseau, 2018; Goedert, Eisenberg, et al., 2017; Guo & Lee, 2014).

Inhibition of tau aggregation and propagation might be the good therapeutic strategy. Inhibition of tau hyperphosphorylation or interaction with tau can be used to prevent aggregation. Transmission routes should cut off to prevent propagation. One key step relies on receptormediated uptake, such as that involving heparan sulfate (HS) proteoglycans (PGs). In a previous study (Zhao et al., 2020), 3-O-sulfation of HS was shown to enhance tau interaction and cellular uptake, suggesting that mimics of HS might also be good candidates for the inhibition of tau aggregation and propagation.

There are three typical marine algae, brown, green and red algae. Sulfated polysaccharides are distributed among these. For example, sulfated xylogalactoarabians (with a backbone of 4-linked or 5-linked arabinopyranose residues sulfated at C3, 3-linked or 6-linked galactopyranose residues sulfated at C4 or C6, and 4-linked xylopyranose residues) and sulfated glucuronoxylorhamnans (with a backbone of 4linked rhamnopyranose sulfated at C3 or C2, 4-linked glucuronic acid residue and 4-linked xylopyranose residue) are from green algae (Arata, Quintana, Raffo, & Ciancia, 2016; Lahaye & Robic, 2007). Fucoidans are from brown algae. According to a previous review (Deniaud-Bouet, Hardouin, Potin, Kloareg, & Herve, 2017), fucoidans can be divided into two types: one had backbone structures based on fucopyranosyl residues (called sulfated galactofucan/fucan in this study), another has backbone structures based on a variety of glycosyl residues (called heteropolysaccharides in this study, including sulfated fucoglucuronan, fucoglucuronomannan, etc.), most of which contain glucuronic acid. Many studies had reported the biological activities of fucoidans, such as anticancer activities, anti-inflammatory activities and immunomodulatory activities (Cumashi et al., 2007; Senthilkumar, Manivasagan, Venkatesan, & Kim, 2013; Wijesinghe & Jeon, 2012).

We speculate that these polysaccharides might compete with HS to bind tau, resulting in cessation of tau spreading. To test this hypothesis, sixty fucoidans/glycans with different structural determinants that had previously prepared were studied. For example, one crude polysaccharide from Enteromorpha prolifera (green algae) extracted by hot water extraction (EP), one crude polysaccharide from Saccharina japonica (brown algae) by hot water extraction (SJ), and three crude polysaccharides from Sargassum thunbergii (brown algae) by hot water extraction (SJW), dilute acid extraction (STA) and dilute alkali extraction (STJ) were previously prepared (Jin et al., 2017; Jin, Zhang, Liang, & Zhang, 2016). Anion exchange chromatography was performed to separate the crude polysaccharides into three fractions (W-type fraction: 0.5 M NaCl fraction; I-type fraction: 1.0 M NaCl fraction; S-type fraction: 2.0 M fraction) to further confirm the active constituents. In addition, considering the effects of molecular weight, acid degradation by HCOOH combined with ultrafiltration devices (Ultracel 100 kDa membrane, Ultracel 50 kDa membrane, Ultracel 30 kDa membrane, Ultracel 10 kDa membrane and Ultracel 3 kDa membrane) were performed to separate the crude polysaccharides into five fractions (fraction 100K, 50K, 30K, 10K and 3K). Acid degradation with 0.1 M HCl and 0.5 M HCl combined with ethanol precipitation were used to obtained three fractions (dilute acid-sensitive fraction (SJ-GX-1), acid-sensitive fraction (SJ-GX-2) and acid-stable fraction (SJ-GX-3)). Oxidative degradation by H₂O₂/ascorbic acid was performed to obtain low molecular weight fractions (SJ-D) (Jin et al., 2013). Moreover, autohydrolysis of sulfated galactofucans (SJ-D-I and SJ-D-S) was used to selectively remove the 2sulfate ester from fucopyranose (Fuc) residues or galactopyranose (Gal) residues to obtain two types of fractions, including larger molecular weight fraction (fraction H) and low molecular weight fraction (fraction

L) (Jin, Jiang, Zhang, et al., 2020; Jin, Zhang, Mitra, et al., 2020). Finally, glucuronomannan oligomers (G2, G4 and G6, corresponding to disaccharide, tetrasaccharide and hexasaccharide, respectively) and glucuronomannan polysaccharide (Gn) with a molecular weight of 7.0 k Da were previously prepared (Jin, He, Zhu, et al., 2020).

Surface plasmon resonance (SPR) solution competition studies were performed to test the binding abilities of these polysaccharides to tau. In addition, NMR titration and cellular uptake assay were performed to map the binding sites and confirm the inhibition of tau spreading.

2. Materials and methods

2.1. Materials

The fucoidans and their derivatives were previously prepared in our lab and are summarized in Table S1. Recombinant tau protein was expressed in *Escherichia coli* BL21-DE3 cells with plasmids for tau441 (gifts from Dr. David Eliezer) and were prepared according to the previous studies (Details in the supplementary data). The method of NMR titration is also presented in the supplementary data.

2.2. Solution competition study between heparin on chip surface and polysaccharides in solution using SPR

SPR was performed on a BIAcore 3000 (GE Healthcare, Uppsala, Sweden). Heparin chip was prepared in the previous studies (Zhang et al., 2019; Zhao et al., 2017) by the immobilization of biotinylated heparin on a streptavidin (SA) chip. Recombinant tau protein was premixed with different concentrations of samples and injected over the heparin chip at the flow rate of 30 $\mu L/min$ to determine the inhibition of samples on tau protein binding to the surface heparin. A dissociation period and regeneration with 2 M NaCl was used after each run.

2.3. Solution competition study using amplified luminescent proximity homogenous assay linked immunosorbent assay (AlphaLISA)

We performed the competition study using AlphaLISA with different beads. Briefly, 2 μL of Streptavidin AlphaLISA® Acceptor beads (Dilute to 100-fold) were added into 10 μL of AlphaLISA HiBlock Buffer (Dilute to 10-fold). Then, 2 μL of 1 μM biotinylated heparin, 2 μL of different concentrations of samples or buffer as a control and 2 μL of 1 μM His-tau protein and 2 μL of Nickel Chelate Alpha Donor beads (dilute to 100-fold) were added sequentially. After a 1 h incubation, the plate was read on an infinite M1000 PRO at 680 nm and 615 nm wavelengths for excitation and detection, respectively. The inhibition was calculated by the equation as follows: Inhibition (%) = (1 - N/N0) \times 100, where N is the data of samples and N0 is the data of control.

2.4. Endothelial cell surface tau binding assay

Mouse lung endothelial cells at 80 % confluent were trypsinized and seeded at 30,000/well in a 96-well plate one day before the assay. The assay was carried out at room temperature. During the assay, the cells were washed with DPBS, fixated with 4 % PFA, further washing with DPBS, and then blocked with blocking buffer (DPBS containing 1 % BSA) for 2 h. The fixed cells were incubated at 4 °C overnight with biotinylated tau (200 ng/well) or biotinylated tau (200 ng/well) mixed with heparin (20 µg/well), SJ-D-I-H (20 µg/well), SJ-GX-3 (20 µg/well), SJ-I (20 µg/well) or SJ-D-I (20 µg/well) (100 µL/well) in the blocking buffer. After washing with DPBS, incubation with Strepadvin-HRP at 1:2000 dilution for 1 h and further extensive washing with DPBS, the tau that bound on the endothelial cell surface was measured using 1-StepTM Ultra TMB-ELISA Substrate Solution (ThermoFisher Scientific, Catlog No. 34028) according to the manufacturer's protocol.

2.5. Tau uptake assay

Mouse lung endothelial cells at 80 % confluent were trypsinized and seeded onto coverslips 24-well plate at 40,000/well one day before the assay. During the assay, after washing with DPBS, the cells were incubated with tau-AF488 (25 $\mu g/mL$) or tau-AF488 (25 $\mu g/mL$) mixed with heparin, SJ-D-I-H, SJ-GX-3, SJ-I or SJ-D-I (25 $\mu g/mL$) at 37 °C, 5 % CO₂ for 3 h. Following, the cells were washed with DPBS, fixed with 4 % PFA at room temperature for 15 min and further washing with DPS, and then the coverslips were picked up, placed on a slide, and mounted with mounting medium contain DAPI. The internalized tau and cell nucleus were imaged under confocal microscope (Zeiss LSM 880 Microscope). The acquired data were processed and quantified using Image J.

3. Results and discussion

3.1. The binding abilities of polysaccharides to tau protein by SPR and AlphaLISA

The binding abilities of five crude polysaccharides (STW, STA, STJ, SJ and EP) were determined by competition SPR (Fig. 1). STW, STA, STJ and SJ were extracted from brown alga while EP was extracted from green alga. Crude polysaccharides showed stronger binding abilities to tau than heparin. Therefore, anion exchange chromatography was performed to separate the crude polysaccharides into three fractions (Wtype fraction: 0.5 M NaCl fraction; I-type fraction: 1.0 M NaCl fraction; S-type fraction: 2.0 M fraction), and the S-fraction exhibited the strongest binding abilities. In addition, crude polysaccharides were degraded by 0.2 M HCOOH, then the degraded solutions were separated by ultrafiltration devices (Ultracel 100 kDa membrane, Ultracel 50 kDa membrane, Ultracel 30 kDa membrane, Ultracel 10 kDa membrane and Ultracel 3 kDa membrane) into five fractions (100K-type fraction: 100K cut-off; 50K-type fraction: 50K cut-off; 30K-type fraction: 30K cut-off; 10K-type fraction: 10K cut-off; 3K-type fraction: 3K cut-off). The results of the binding abilities of the fractions showed that the larger the molecular weight of polysaccharides were, the stronger the binding affinities were, except for STW-100K, STA-100K and STJ-100K. It is interesting to note that the fractions from SJ showed the stronger

binding abilities than other fractions from STW, STA, STJ and EP. According to previous studies (Deniaud-Bouet et al., 2017; Jin et al., 2013; Jin et al., 2016; Jin et al., 2017), W-type fractions from STW, STA, STJ and SJ were heteropolysaccharides, containing galactan, glucuronan and glucuronomannan while I-type fractions and S-fractions were mainly sulfated fucan/galactofucan. EP was mainly a sulfated glucurono-xylo-rhamnan (Jin, He, Long, et al., 2020), however, the inhibitions of binding affinities were lower than the corresponding fractions from STW, STA, STJ and SJ. Therefore, the fractions were considered for further studies. Finally, SJ and its fractions were chosen for the candidates to determine their binding affinities with tau.

SJ was degraded by H_2O_2 /ascorbic acid to obtain low molecular weight SJ (SJ-D) and SJ-D was performed on anion exchange chromatography to obtain SJ-D-W, SJ-D-I and SJ-D-S (Jin et al., 2013) to examine the influence of molecular weight on binding. SPR results indicated that the binding abilities of SJ-D to tau was lower than SJ, suggesting that molecular weight was important, which are consistent with the above results. In addition, SJ-D-I and SJ-D-S showed stronger binding abilities than SJ-D-W. In a previous study (Jin et al., 2013), both SJ-D-I and SJ-D-S were shown to correspond to the major sulfated galactofucan. Autohydrolysis of sulfated galactofucans (SJ-D-I and SJ-D-S) was used to selectively remove the 2-sulfate ester from fucopyranose (Fuc) residues or galactopyranose (Gal) residues (Jin, Jiang, Zhang, et al., 2020; Jin, Zhang, Mitra, et al., 2020) and products were separated into two fractions: the high molecular weight fraction (SJ-D-I-H and SJ-D-S-H) and the low molecular weight fraction (SJ-D-I-L and SJ-D-S-L). Solution competition studies were performed by surface plasmon resonance (SPR) to determine the effects of these four sulfated galactofucans, as shown in Fig. S1. SJ-D-I-H and SJ-D-S-H exhibited stronger binding abilities than SJ-D-I-L and SJ-D-S-L. In addition, the normalized tau binding abilities of SJ-D-I-H and SJ-D-S-H were both 12 %, compared with SJ-D-I (5 %) and SJ-D-S (9 %), suggesting that 2-sulfation of sulfated galactofucan might not be important. Therefore, SJ-I was chosen for the next study. SJ-I produced the strongest inhibition (>97 %) in competing for tau protein binding to immobilized heparin, followed by SJ-D-I (approximately 95 %) and SJ-D-I-H (approximately 88 %), and SJ-D-I-L showed modest inhibitory activity (approximately 74 %), which was lower than heparin (approximately 80 %). It is possible that

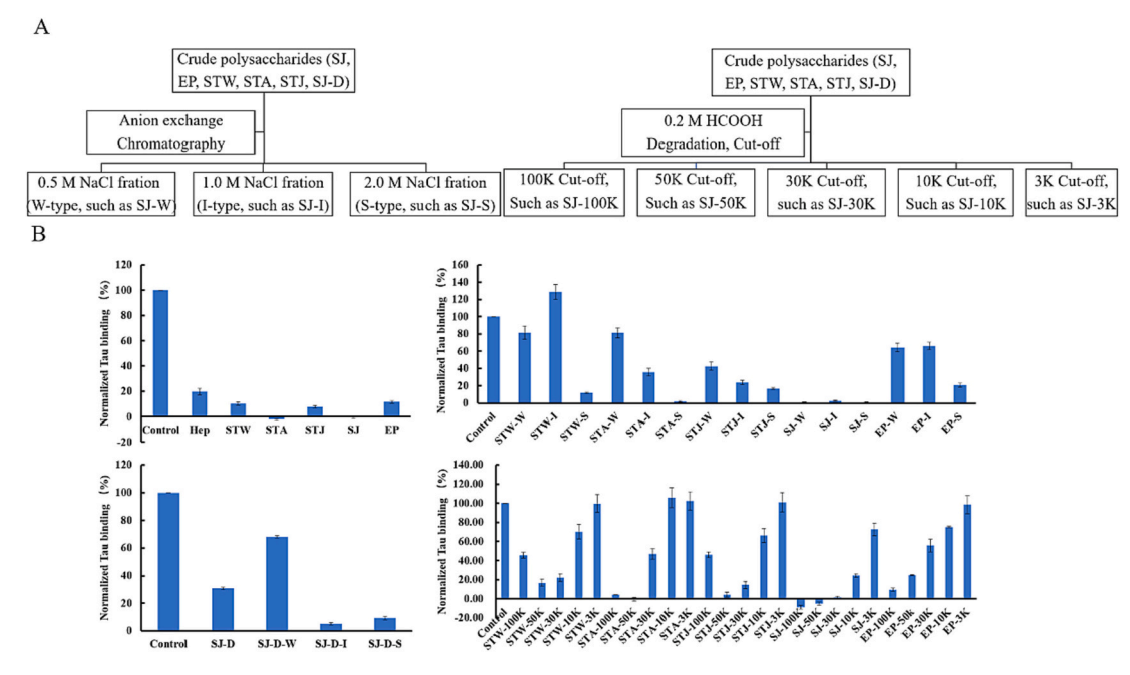


Fig. 1. Inhibition abilities of crude polysaccharides and their fractions on tau-heparin interactions determined by SPR (A): preparation process of polysaccharide preparation; (B): bar graphs of normalized tau binding preference to surface heparin by competing with different polysaccharides in solution. Concentrations were 150 nM for tau, and concentrations of different polysaccharides were 1000 nM. All bar graphs based on triplicate experiments.

the molecular weight and 2-sulfation of Fuc residues influence the binding ability, however, the effects are not significant because SJ-D-I-H retained the binding activity of SJ-I. Kinetic measurements of tau to SJ-I, SJ-D-I and SJ-D-I-H interaction were further determined by solution-based affinities (Ki), using the equation: Ki = IC₅₀ / (1 + [C] / K_D), where IC₅₀ value measured from SPR competition experiments, [C] is the concentration of tau (150 nM) used in the competition SPR, and K_D is the tau-heparin binding affinity (K_D = 20 nM) according to the previous studies (Zhao et al., 2020). The IC₅₀ values of SJ-I, SJ-D-I and SJ-D-I-H were 15, 45 and 32 nM, as shown in Fig. 2B–D. Therefore, the Ki of SJ-I, SJ-D-I and SJ-D-I-H were 1.8, 5.3 and 3.8 nM, respectively, suggesting that SJ-I, SJ-D-I and SJ-D-I-H showed stronger inhibitory activities than did heparin. However, the IC₅₀ values for heparin, SJ-I, SJ-D-I and SJ-D-I-H were 0.92, 0.15, 2.57 and 5.02 μ M using AlphaLISA in Fig. 3A–D.

3.2. The binding abilities and sites of sulfated galactofucans to tauK18 protein by NMR

Tau protein is a microtube-associated protein (MAP) that displays various functions in microtube nucleation, assembly, and stabilization (Barré & Eliezer, 2013). Tau protein, including six different isoforms (htau40, htau34, htau24, htau39, htau37 and htau23), is present principally found in axons of the central nervous systems (Andreadis, Brown, & Kosik, 1992; Barré & Eliezer, 2013; Cleveland, Hwo, & Kirschner, 1977a, 1977b; Goedert, Spillantini, Jakes, Rutherford, & Crowther, 1989). The primary sequence of tau protein indicates that it has an Nterminal domain (alternatively spliced exons 2, 3 and 10), two prolinerich domains (P1 and P2) and a C-terminal domain, including the microtube-binding repeats (R1-R4) and the pseudorepeat R' (Barré & Eliezer, 2013). The microtube-binding domain (MBD) contains the proline-rich domains and the microtube-binding repeats, however, only the microtube-binding domains (R1-R4) have the ability to bind

microtubes and to promote their assembly (Trinczek, Biernat, Baumann, Mandelkow, & Mandelkow, 1995). There are two forms of the microtube-binding domains, including K18 (R1-R4) and K19 (R1, R3 and R4). Here, tau K18 was used to study the binding sites of three different sulfated galactofucans (SJ-I, SJ-D-I and SJ-D-I-H) to tau protein. They were individually added into ¹⁵N labeled tau K18 and the refocused two-dimensional ¹H—¹⁵N heteronuclear single quantum coherence (HSQC) NMR spectra were recorded, after the addition of the sulfated galactofucans with two different molar ratios [blue peaks for the molar ratio of sulfated galactofucan to ¹⁵N labeled tau K18 (0.2) and gold peaks for the molar ratio of sulfated galactofucan to $^{15}\mathrm{N}$ labeled tau K18 (0.5)]. Significant chemical shift perturbations (CSPs) in tau protein were detected. The CSPs of SJ-I at two different molar ratios of 0.2 and 0.5 show no significant difference in Fig. 4A and F, suggesting that SJ-I displayed strong binding affinity at the molar ratio of 0.2. The CSPs of SJ-D-I were larger than SJ-D-I-H's CSPs in Fig. 4B, C, G and H, suggesting that SJ-D-I had stronger binding ability than SJ-D-I-H. Comparison of SJ-I, SJ-D-I and SJ-D-I-H in Fig. 4D and E, show that the order of CSPs values is SJ-I > SJ-D-I > SJ-D-I-H, except for some amino acid residues, like L282. The order of binding ability is SJ-I > SJ-D-I > SJ-D-I-H, consistent with the AlphaLISA results. Significant CSPs are located at R2 domains, in which residues I278 and N279 exhibited the two largest CSPs at the molar ratio of 0.2 while I278 and L282 exhibited the two largest CSPs, followed by residue N279 and residue D283 in Fig. 4I-L. It has been reported that the hexapeptide ²⁷⁵VQIINK²⁸⁰ (PHF6*) in R2, as the main sites of contact with heparin, contributes to tau aggregation and microtubes association (Smet et al., 2004; Zhao et al., 2017; Zhao et al., 2020). It is interesting to note that SJ-D-I and SJ-D-I-H has the largest CSPs at residue L282, while SJ-I shows low CSPs, suggesting that molecular weight and sulfation patter of sulfated galactofucan need to be considered when binding to residue L282. The major similarity between sulfated galactofucan and heparin is the sulfate group. We hypothesized that PHF6* region of repeat 2 (G273-D283) might interact

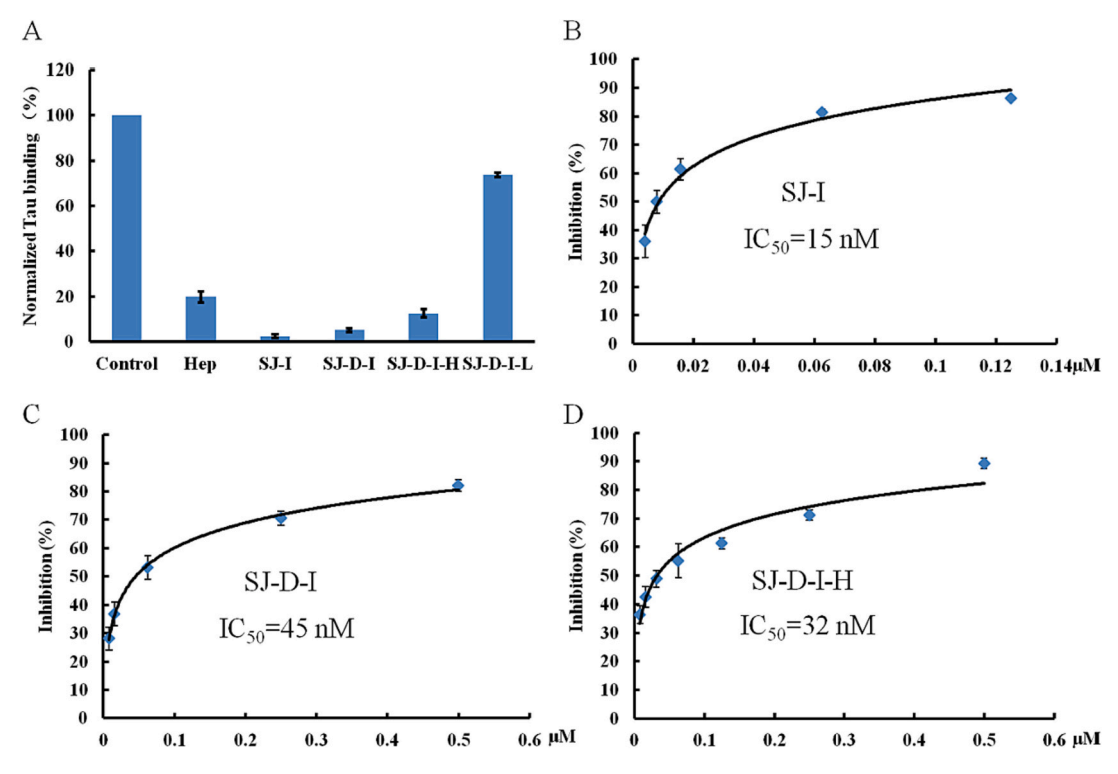


Fig. 2. Inhibition abilities of SJ-I, SJ-D-I and SJ-D-I-H on tau-heparin interactions determined by SPR and AlphaLISA (A): bar graphs of normalized tau binding preference to surface heparin by competing with different polysaccharides in solution. Concentrations were 150 nM for tau, and concentrations of different polysaccharides were 1000 nM. All bar graphs based on triplicate experiments; (B): the IC_{50} of SJ-I; (C): The IC_{50} of SJ-D-I and (D): The IC_{50} of SJ-D-I-H. Concentrations were 150 nM for tau. All bar graphs based on triplicate experiments; The binding ability of Heparin (E), SJ-I (F), SJ-D-I (G) and SJ-D-I-H (H) to tau determined by AlphaLISA. All bar graphs based on triplicate experiments.

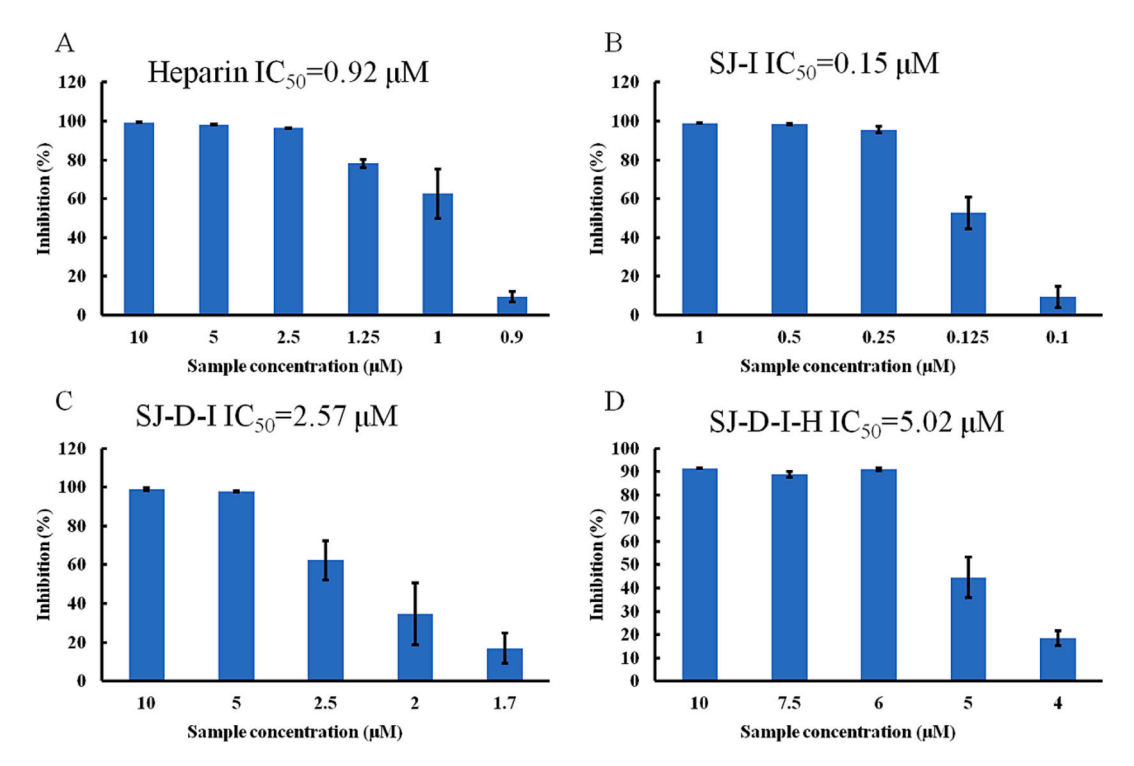


Fig. 3. Inhibition abilities of SJ-I, SJ-D-I and SJ-D-I-H on tau-heparin interactions determined by AlphaLISA. The binding ability of Heparin (A), SJ-I (B), SJ-D-I (C) and SJ-D-I-H (D) to tau determined by AlphaLISA. All bar graphs based on triplicate experiments.

with sulfate group. We observe some large CSPs in the N-terminal region of R1, however, it has been reported that R1 unlikely participate in nucleating beta-sheet formation because of the presence of several proline residues (Mukrasch et al., 2005). The Module-B region (V337-K343) in the N-terminal region of R4 plays an important modulator of tau filament morphology, however, it does not significantly decrease tau filament formation (DeTure, Di Noto, & Purich, 2002). It has been shown (Barré & Eliezer, 2013) that PHF6 hexapeptide (V306-D314) region of R3 are more effective than PHF6* and Module-B in nucleating tau aggregation. In Fig. 4D that the CSPs in the PHF6 of SJ-I were higher than SJ-D-I's and SJ-D-I-H's, explaining the reason why SJ-I had higher binding ability than SJ-D-I's and SJ-D-I-H's. Therefore, we conclude that the decreasing of molecular weight and 2-sulfation of Fuc residues reduces to a certain extent of the binding affinity of sulfated galactofucans.

3.3. The binding abilities of heteropolysaccharide to tau protein by SPR and AlphaLISA

Polysaccharides containing uronic acid are more stable under acidic conditions, suggesting that 100K-type fractions and 50K-type fractions are mainly heteropolysaccharides containing uronic acid. However, inconsistent with the above results the binding affinities of W-type fractions (mainly heteropolysaccharides) are lower than I-type and Stype fractions. Therefore, we propose that high molecular weight heteropolysaccharides but not low molecular weight heteropolysaccharides contribute to the binding affinities to tau. SJ was degraded by 0.1 M HCl and precipitated by ethanol to obtain two fractions, the supernatant (SJ-GX-1) and the precipitation to confirm this hypothesis. Finally, the precipitant was degraded again with 0.5 M HCl and then precipitated by ethanol to obtain two fractions, the supernatant (SJ-GX-2) and the precipitation (SJ-GX-3). The preparation of SJ-GX-1, SJ-GX-2 and SJ-GX-3 is summarized in Fig. 5A. SJ-GX-3 (heteropolysaccharide) was the most stable fraction and might have similar backbone structures to 100K-type fractions and 50K-type fractions. Surface competition experiments were performed by SPR to examine the effects of SJ and its derivates (SJ-GX-1, SJ-GX-2 and SJ-GX-3) on the tau-heparin

interaction in Fig. 5B. SJ-GX-3 exhibited the strongest inhibitory activity, similar to SJ, followed by SJ-GX-1 and SJ-GX-2. The IC $_{50}$ of SJ-GX-3 was determined by two different methods, SPR and Alphascreen. The IC $_{50}$ was 13 nM by SPR and 0.24 μ M by Alphascreen (Fig. 5C and D). Glucuronomannan (Gn) is a major fraction of heteropolysaccharide, so Gn (7.0 kDa) and its oligomers (dimer (G2), tetramer (G4) and hexamer (G6)) were prepared (Jin, He, Zhu, et al., 2020). These oligomers did not show the tau binding affinity, while Gn exhibited lower similar binding affinity than SJ-GX-3, confirming that molecular weight contributed to the binding affinity of heteropolysaccharides to tau.

3.4. The binding abilities and binding sites of SJ-GX-3 to tauK18 protein by NMR

Based on the results of SPR and Alphascreen, we conclude that the binding affinity of SJ-GX-3 was lower than that of SJ-I, but higher than those of SJ-D-I and SJ-D-I-H. SJ-GX-3 has a backbone of Gn and/or glucuronan while SJ-I has a backbone of fucan and/or galactofucan, suggesting that they have different structures. We asked whether they have similar binding site to tau K18. Tau K18 was used to study the binding sites of SJ-GX-3 to tau protein (Fig. 6). Comparing SJ-GX-3 with SJ-I, SJ-D-I and SJ-D-I-H at the molar ratio of 0.2, we find that most CSPs of SJ-GX-3 were between SJ-I and SJ-D-I, consistent with the results of SPR and Alphascreen. It also indicates that these binding sites might be the binding regions between fucoidans and tau K18. It is interesting to note that the CSPs of SJ-GX-3 at the residues H268, L282 and H299 are higher than SJ-I's, suggesting that these residues might be the characteristic binding regions for Gn or glucuronan.

3.5. Sulfated galactofucan and SJ serial fraction preparations inhibit tau cell surface binding and cellular uptake

We recently reported that HS essentially mediated mouse lung endothelial cell surface tau binding and the subsequent uptake (Zhao et al., 2020). Therefore, we further tested if the serial SJ fractions could function as inhibitors to block the HS-mediated processes. As expected,

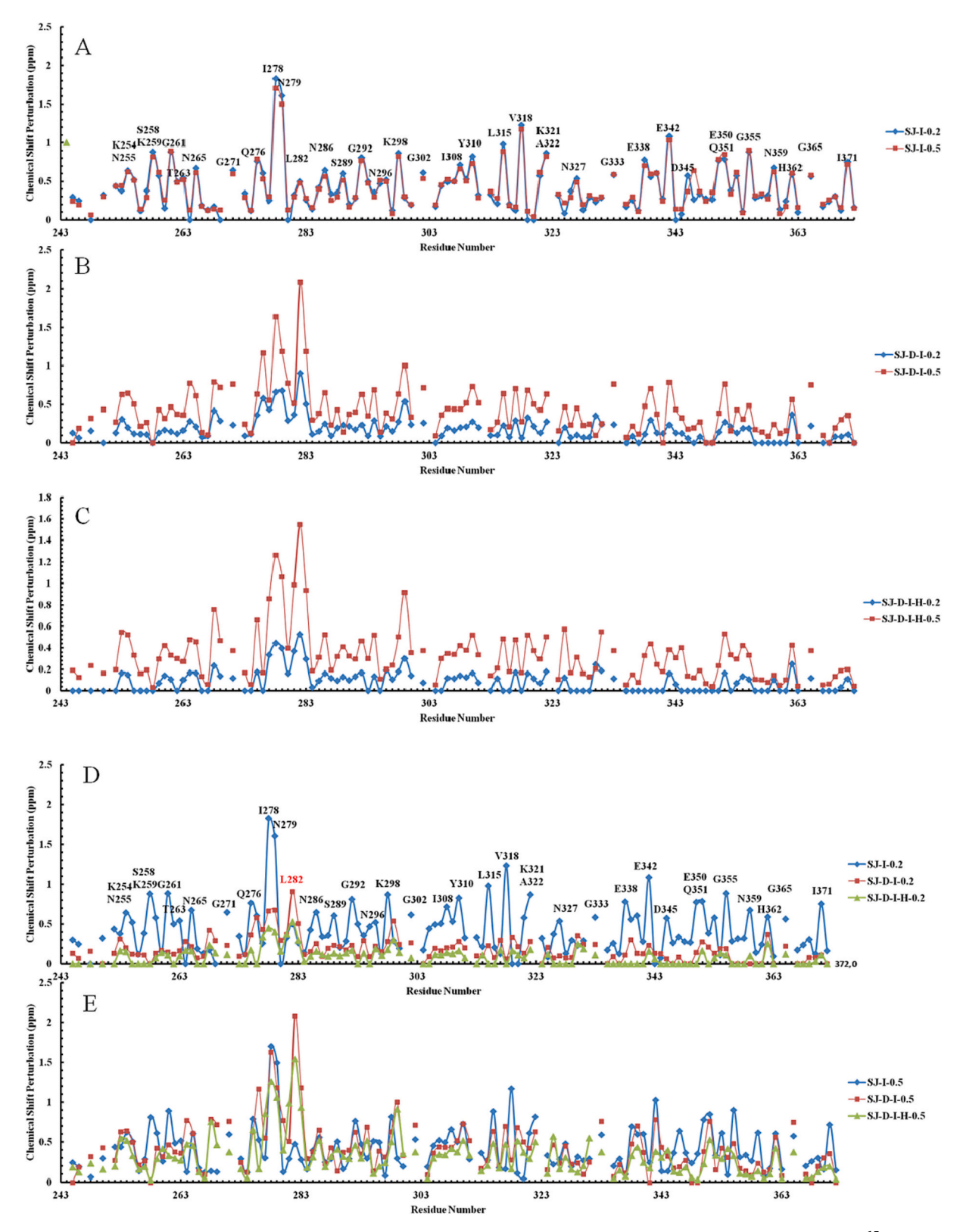


Fig. 4. Chemical shift perturbation (CSP) difference reveals specific interactions between polysaccharides (SJ-I, SJ-D-I and SJ-D-I-H) and ¹⁵N tau K18. (A) CSP differences of two different molar ratios of SJ-I (SJ-I-0.2 means that the molar ratio of SJ-I to ¹⁵N tau K18 was 0.2 while SJ-I-0.5 means that the molar ratio of SJ-I to ¹⁵N tau K18 was 0.5); (B) CSP differences of two different molar ratios of SJ-D-I-H; (C) CSP differences of two different molar ratios of SJ-D-I-H; (D) CSP differences of SJ-I-0.2, SJ-D-I-0.2 and SJ-D-I-H-0.2; (E) CSP differences of SJ-I-0.5, SJ-D-I-0.5 and SJ-D-I-H-0.5; (F) overlay of ¹H—¹⁵N HSQC spectra of ¹⁵N tau K18 before (red) and after 0.2 molar ratio addition of SJ-I (blue) and 0.5 molar ratio addition of SJ-D-I (gold); (H) overlay of ¹H—¹⁵N HSQC spectra of ¹⁵N tau K18 before (red) and after 0.2 molar ratio addition of SJ-D-I (blue) and 0.5 molar ratio addition of SJ-D-I (gold); (I) overlay of ¹H—¹⁵N HSQC spectra of ¹⁵N tau K18 before (red) and after 0.2 molar ratio addition of SJ-D-I-H (blue) and 0.5 molar ratio addition of SJ-D-I-H (gold); (I) zoomed-in NMR spectrum at residue I278 of SJ-D-I-H with high CSPs; (J) zoomed-in NMR spectrum at residue D283 of SJ-D-I-H with high CSPs; (L) zoomed-in NMR spectrum at residue D283 of SJ-D-I-H with high CSPs.

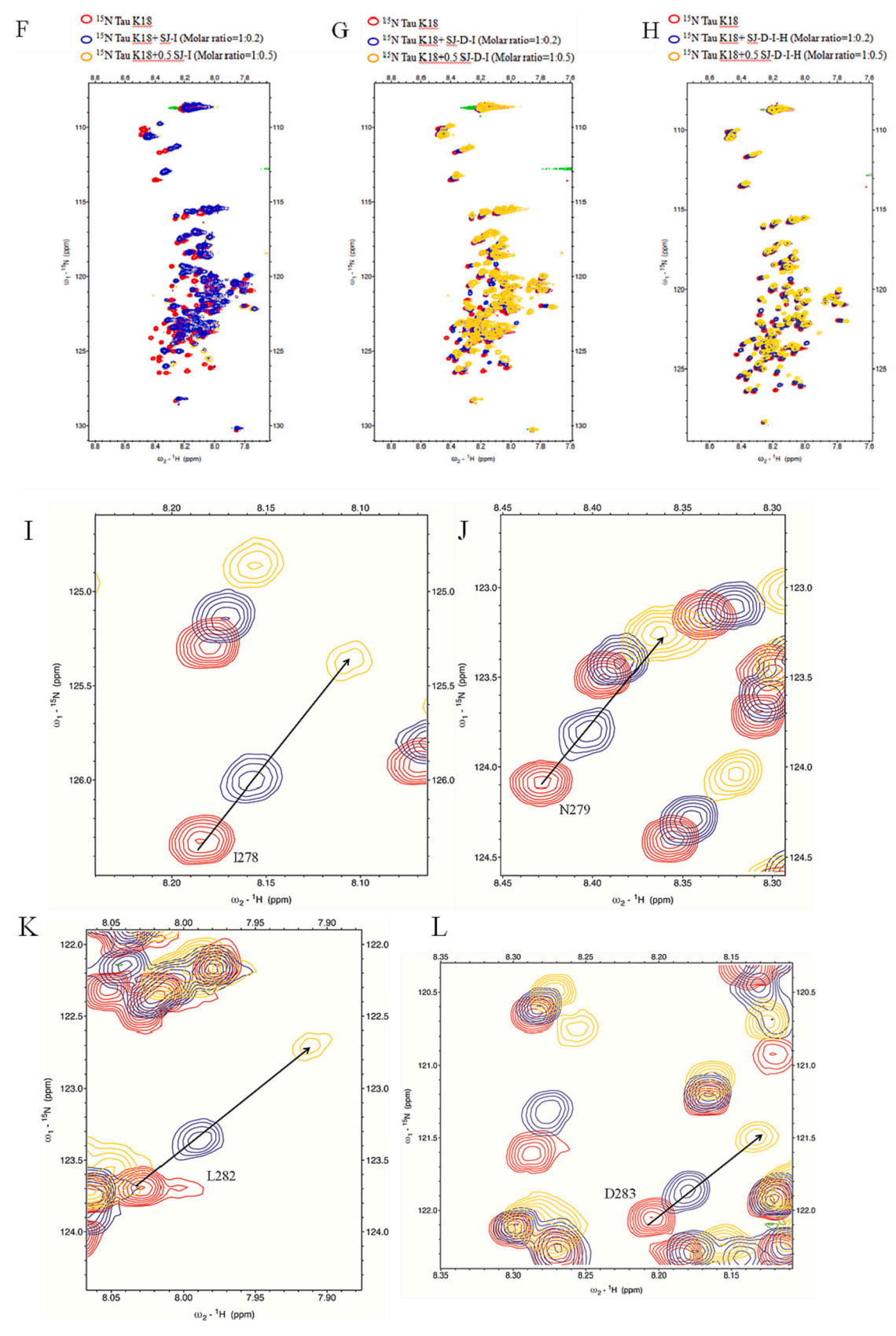


Fig. 4. (continued).

mouse lung endothelial cells surface showed a strong cell surface tau binding and intracellular uptake, and the two processes were effectively blocked by heparin at 20 μ g/mL and 25 μ g/mL, respectively (Fig. 7). The

SJ fraction preparations, including SJ-I, SJ-D-I, SJ-D-I-H and SJ-GX-3 (The structures of these polysaccharides were summarized in Fig. 7C), were tested at the same concentrations in the two assays and potently

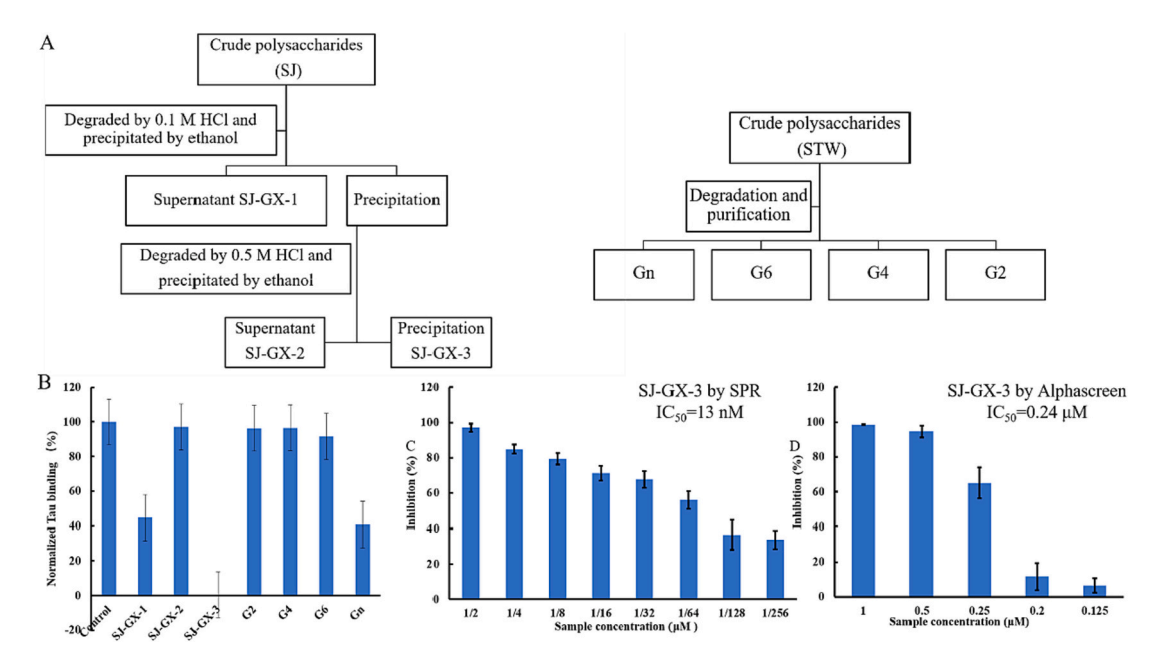


Fig. 5. Inhibition abilities of polysaccharides on tau-heparin interations determined by SPR and Alphascreen (A): the flow chart of the polysaccharide preparation; (B): bar graphs of normalized tau binding preference to surface heparin by competing with SJ-GX-1, SJ-GX-2 and SJ-GX-3 in solution. Concentrations were 150 nM for tau, and concentrations of different polysaccharides were 1000 nM. All bar graphs based on triplicate experiments; (C): the IC_{50} of SJ-GX-3 determined by SPR; concentrations were 150 nM for tau, and concentrations of different polysaccharides were 1000 nM. All bar graphs based on triplicate experiments; (D): the IC_{50} of SJ-GX-3 determined by Alphascreen. All bar graphs based on triplicate experiments.

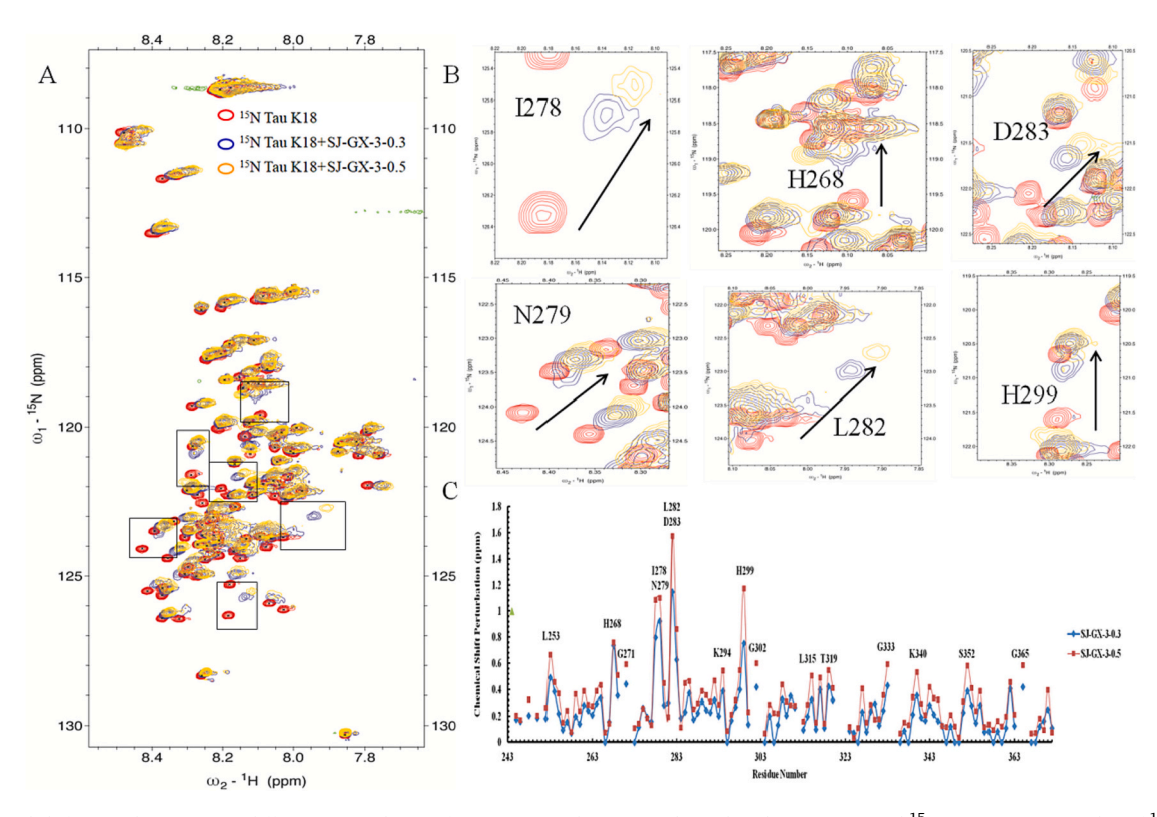


Fig. 6. Chemical shift perturbation (CSP) difference reveals specific interactions between polysaccharide (SJ-GX-3) and ¹⁵N tau K18. (A) Overlay of ¹H—¹⁵N HSQC spectra of ¹⁵N tau K18 before (red) and after 0.3 molar ratio addition of SJ-I (blue) and 0.5 molar ratio addition of SJ-I (gold); (B) zoomed-in NMR spectra at residue I278, H268, D283, N279, L282 and H299 of SJ-GX-3 with high CSPs; (C) CSP differences of two different molar ratios of SJ-GX-3 (SJ-GX-3-0.3 means that the molar ratio of SJ-GX-3 to ¹⁵N tau K18 was 0.3 while SJ-GX-3-0.5 means that the molar ratio of SJ-GX-3 to ¹⁵N tau K18 was 0.5).

blocked tau cell surface binding and the intracellular internalization too, with their inhibitory activities comparable to even slightly higher than heparin (Fig. 7).

4. Conclusion

The spread of tau pathology is a phenomenon in the earliest phase of

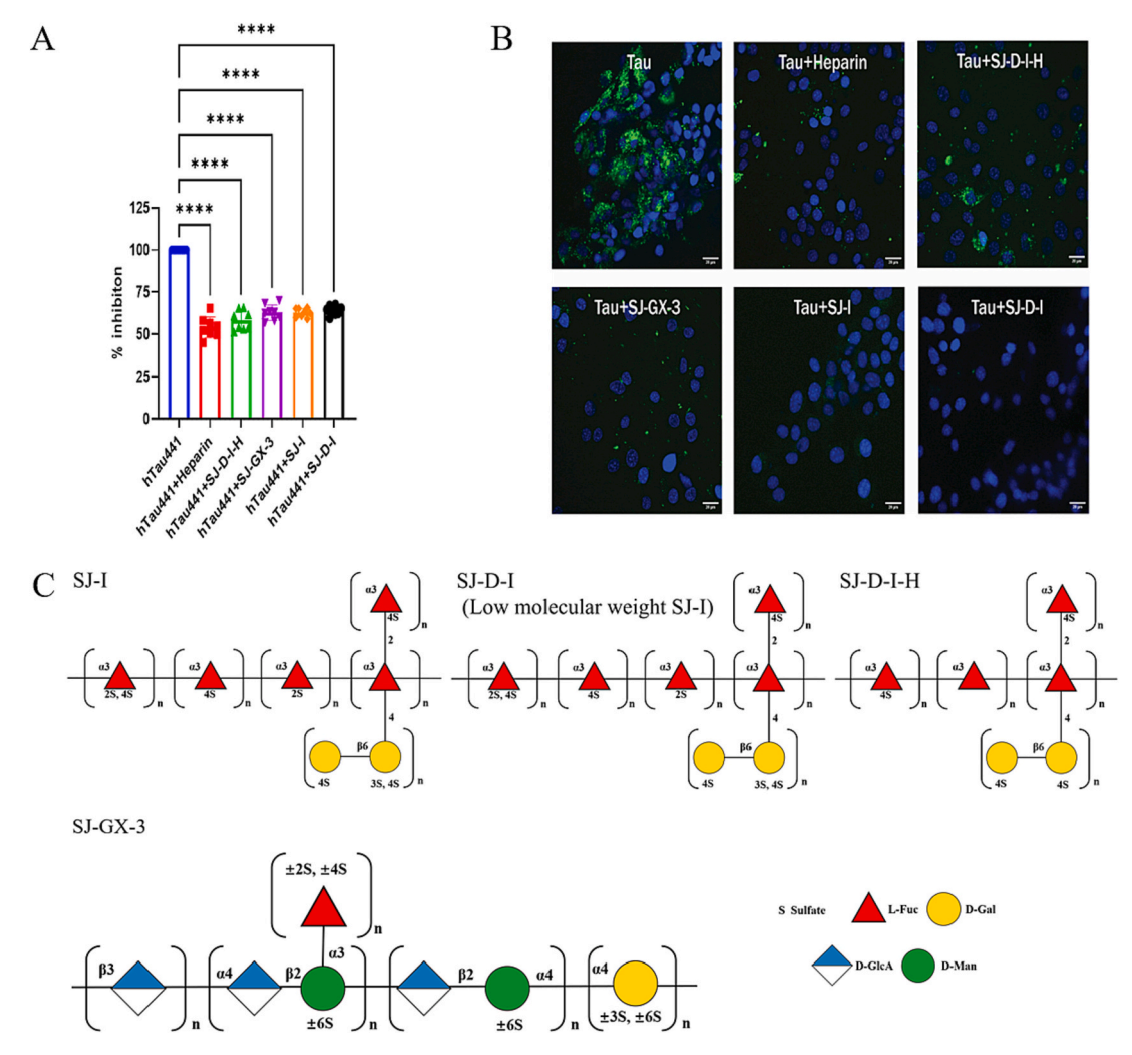


Fig. 7. Sulfated galactofucans and SJ-GX-3 inhibited tau-cell surface binding and cellular uptake. A. Heparin (HP), SJ-D-I-H, SJ-GX-3, SJ-I and SJ-D-I inhibit tau cell surface binding by 54.1 %, 58.3 %, 62.9 %, 62.8 % and 63.9 %, respectively. After fixing and incubating with biotinylated tau (200 ng/well, 100 μ L/well) without or with HP (20 μ g/well), SJ-I, SJ-D-I, SJ-D-I-H and SJ-GX-3 (20 μ g/well) for 90 min at RT, the cell surface bound biotin-tau was measured by incubating with Streptavidin-HRP and color development. B. (Right) HP, SJ-I, SJ-D-I-H and SJ-GX-3 inhibit tau internalization as assessed by confocal images. The cells were incubated with tau-Alexa (25 μ g/mL, 500 μ L/well) without or with HP (25 μ g/mL), SJ-I, SJ-D-I-H and SJ-GX-3 (25 μ g/mL) at 37 °C for 3 h and then imaged after washing with PBS and fixing with 4 % PFA. The data shown are representative of 2–4 independent experiments. C. Proposed primary structures of SJ-I, SJ-D-I-H, SJ-GX-3 and SJ-D-I.

Alzheimer's disease and tau spreading is mediated by cell surface HS. Therefore, one promising pharmacological treatment might be to find a competitor to bind tau. Fucoidans exhibited stronger binding affinity to tau than heparin. Two major fractions of fucoidans-sulfated galatofucan and sulfated heteropolysaccharides, were the main components. Cell surface tau binding assay and tau internalization assay confirmed that these two fractions exhibited similar activities as heparin. In addition, the molecular weight and 2-sulfation of fucoidans contribute to binding affinity. Finally, NMR titration assay indicates that the binding regions of sulfated galactofucan and sulfated heteropolysaccharides provide a theoretical basis for the design of tau spreading inhibitors.

CRediT authorship contribution statement

Weihua Jin: Conceptualization, Methodology, Data curation, Formal analysis, Funding acquisition, Resources, Writing-Original draft preparation, Project administration; Chenghui Lu: Conceptualization, Methodology; Yanan Zhu: Conceptualization, Methodology; Jing Zhao: Conceptualization, Methodology; Wenjing Zhang: Methodology, Writing-Original draft preparation, Funding acquisition; Lianchun Wang: Methodology, Writing Reviewing and Editing; Robert J. Linhardt:

Writing-Reviewing, Editing and Funding acquisition; Chunyu Wang: Methodology, Writing Reviewing, Editing, and Funding acquisition; Fuming Zhang: Methodology, Writing Reviewing, Editing, and Funding acquisition.

Declaration of competing interest

The authors declare no conflicts of interest.

Data availability

Data will be made available on request.

Acknowledgements

This study was supported by the National Natural Science Foundation of China (No. 41906095 to W.Z.); the Zhejiang Provincial Natural Science Foundation of China (No. LY19D060006 to W.J.); National Institutes of Health (NIH) Grants DK111958 (to R.J.L), and AG069039 (to C. W. and R.J.L); and GlycoMIP a National Science Foundation Materials Innovation Platform funded through Cooperative Agreement DMR-

1933525 (to F. Z. and R.J.L).

Appendix A. Supplementary data

Supplementary data to this article can be found online at https://doi.org/10.1016/j.carbpol.2022.120176.

References

- 2020 2020 Alzheimer's disease facts and figures. (2020). Alzheimers Dement.
- Aging, N. I.o. (2020). https://www.nia.nih.gov/health/alzheimers/basics.
- Andreadis, A., Brown, W. M., & Kosik, K. S. (1992). Structure and novel exons of the human tau gene. *Biochemistry*, *31*(43), 10626–10633.
- Arata, P. X., Quintana, I., Raffo, M. P., & Ciancia, M. (2016). Novel sulfated xylogalactoarabinans from green seaweed Cladophora falklandica: Chemical structure and action on the fibrin network. *Carbohydrate Polymers*, 154, 139–150.
- Ballatore, C., Lee, V. M., & Trojanowski, J. Q. (2007). Tau-mediated neurodegeneration in Alzheimer's disease and related disorders. *Nature Reviews Neuroscience*, 8(9), 663–672.
- Barré, P., & Eliezer, D. (2013). Structural transitions in tau k18 on micelle binding suggest a hierarchy in the efficacy of individual microtubule-binding repeats in filament nucleation. *Protein Science: A Publication of the Protein Society*, 22(8), 1037–1048.
- Brettschneider, J., Del Tredici, K., Lee, V. M., & Trojanowski, J. Q. (2015). Spreading of pathology in neurodegenerative diseases: A focus on human studies. *Nature Reviews Neuroscience*, 16(2), 109–120.
- Cairns, D. M., Rouleau, N., Parker, R. N., Walsh, K. G., Gehrke, L., & Kaplan, D. L. (2020).
 A 3D human brain-like tissue model of herpes-induced Alzheimer's disease. Science Advance, 6, eaay8828.
- Chu, D., & Liu, F. (2019). Pathological changes of tau related to Alzheimer's disease. ACS Chemical Neuroscience, 10(2), 931–944.
- Cleveland, D. W., Hwo, S. Y., & Kirschner, M. W. (1977a). Physical and chemical properties of purified tau factor and the role of tau in microtubule assembly. *Journal* of Molecular Biology, 116(2), 227–247.
- Cleveland, D. W., Hwo, S. Y., & Kirschner, M. W. (1977b). Purification of tau, a microtubule-associated protein that induces assembly of microtubules from purified tubulin. *Journal of Molecular Biology*, 116(2), 207–225.
- Colin, M., Dujardin, S., Schraen-Maschke, S., Meno-Tetang, G., Duyckaerts, C., Courade, J. P., & Buee, L. (2020). From the prion-like propagation hypothesis to therapeutic strategies of anti-tau immunotherapy. *Acta Neuropathologica*, 139(1), 3–25
- Cumashi, A., Ushakova, N. A., Preobrazhenskaya, M. E., D'Incecco, A., Piccoli, A., Totani, L., Tinari, N., Morozevich, G. E., Berman, A. E., Bilan, M. I., Usov, A. I., Ustyuzhanina, N. E., Grachev, A. A., Sanderson, C. J., Kelly, M., Rabinovich, G. A., Lacobelli, S., & Nifantiev, N. E. (2007). A comparative study of the antiinflammatory, anticoagulant, antiangiogenic, and antiadhesive activities of nine different fucoidans from brown seaweeds. Glycobiology, 17(5), 541–552.
- Cummings, J., Lee, G., Ritter, A., & Zhong, K. (2018). Alzheimer's disease drug development pipeline: 2018. Alzheimers Dement (N Y), 4, 195–214.
- Demaegd, K., Schymkowitz, J., & Rousseau, F. (2018). Transcellular spreading of tau in tauopathies. Chembiochem. 19(23), 2424–2432.
- Deniaud-Bouet, E., Hardouin, K., Potin, P., Kloareg, B., & Herve, C. (2017). A review about brown algal cell walls and fucose-containing sulfated polysaccharides: Cell wall context, biomedical properties and key research challenges. *Carbohydrate Polymers*, 175, 395–408.
- DeTure, M. A., Di Noto, L., & Purich, D. L. (2002). In vitro assembly of alzheimer-like filaments. How a small cluster of charged residues in tau and MAP2 controls filament morphology. Journal of biology. *Chemistry*, 277(38), 34755–34759.
- Doig, A. J., Del Castillo-Frias, M. P., Berthoumieu, O., Tarus, B., Nasica-Labouze, J., Sterpone, F., Nguyen, P. H., Hooper, N. M., Faller, P., & Derreumaux, P. (2017). Why is research on amyloid-beta failing to give new drugs for Alzheimer's disease? ACS Chemical Neuroscience, 8(7), 1435–1437.
- Drago, D., Bolognin, S., & Zatta, P. (2008). Role of metal ions in the Aβ oligomerization in Alzheimers disease and in other neurological disorders. *Current Alzheimer Research*, 5(6), 500–507.
- Giacobini, E., & Gold, G. (2013). Alzheimer disease therapy-moving from amyloid- β to tau. Nature Reviews Neurology, 9(12), 677–686.
- Goedert, M., Eisenberg, D. S., & Crowther, R. A. (2017). Propagation of tau aggregates and neurodegeneration. Annual Review of Neuroscience, 40, 189–210.
- Goedert, M., Masuda-Suzukake, M., & Falcon, B. (2017). Like prions: The propagation of aggregated tau and alpha-synuclein in neurodegeneration. *Brain, 140*(2), 266–278.
- Goedert, M., Spillantini, M. G., Jakes, R., Rutherford, D., & Crowther, R. A. (1989). Multiple isoforms of human microtubule-associated protein tau: Sequences and localization in neurofibrillary tangles of Alzheimer's disease. *Neuron*, 3(4), 519–526.
- Guo, J. L., & Lee, V. M. (2014). Cell-to-cell transmission of pathogenic proteins in neurodegenerative diseases. *Nature Medicine*, 20(2), 130–138.

- Herrup, K. (2015). The case for rejecting the amyloid cascade hypothesis. *Nature Neuroscience*, 18(6), 794–799.
- Holmes, B. B., Furman, J. L., Mahan, T. E., Yamasaki, T. R., Mirbaha, H., Eades, W. C.,
 Belaygorod, L., Cairns, N. J., Holtzman, D. M., & Diamond, M. I. (2014).
 Proteopathic tau seeding predicts tauopathy in vivo. Proceedings of the National Academy of Sciences of the United States of America, 111(41), E4376–E4385.
- Ising, C., Venegas, C., Zhang, S., Scheiblich, H., Schmidt, S. V., Vieira-Saecker, A., Schwartz, S., Albasset, S., McManus, R. M., Tejera, D., Griep, A., Santarelli, F., Brosseron, F., Opitz, S., Stunden, J., Merten, M., Kayed, R., Golenbock, D. T., Blum, D., ... Heneka, M. T. (2019). NLRP3 inflammasome activation drives tau pathology. Nature, 575(7784), 669–673.
- Jin, W., He, X., Long, L., Fang, Q., Wei, B., Sun, J., Zhang, W., Wang, H., Zhang, F., & Linhardt, R. J. (2020). Structural characterization and anti-lung cancer activity of a sulfated glucurono-xylo-rhamnan from Enteromorpha prolifera. *Carbohydrate Polymers*, 237, Article 116143.
- Jin, W., He, X., Zhu, J., Fang, Q., Wei, B., Sun, J., Zhang, W., Zhang, Z., Zhang, F., Linhardt, R. J., Wang, H., & Zhong, W. (2020). Inhibition of glucuronomannan hexamer on the proliferation of lung cancer through binding with immunoglobulin G. Carbohydrate Polymers, 248, Article 116785.
- Jin, W., Jiang, D., Zhang, W., Wang, C., Xia, K., Zhang, F., & Linhardt, R. J. (2020). Interactions of fibroblast growth factors with sulfated galactofucan from Saccharina japonica. *International Journal of Biological Macromolecules*, 160, 26–34.
- Jin, W., Zhang, W., Liu, G., Yao, J., Shan, T., Sun, C., & Zhang, Q. (2017). The structureactivity relationship between polysaccharides from Sargassum thumbergii and antitumor activity. *International Journal of Biological Macromolecules*, 105(Part 1), 686–692
- Jin, W., Zhang, W., Mitra, D., McCandless, M. G., Sharma, P., Tandon, R., Zhang, F., & Linhardt, R. J. (2020). The structure-activity relationship of the interactions of SARS-CoV-2 spike glycoproteins with glucuronomannan and sulfated galactofucan from Saccharina japonica. *International Journal of Biological Macromolecules*, 163, 1649–1658.
- Jin, W., Wang, J., Jiang, H., Song, N., Zhang, W. J., & Zhang, Q. B. (2013). The neuroprotective activities of heteropolysaccharides extracted from saccharina japonica. *Carbohydrate Polymers*, 97(1), 116–120.
- Jin, W., Zhang, W. J., Liang, H. Z., & Zhang, Q. B. (2016). The structure-activity relationship between marine algae polysaccharides and anti-complement activity. *Marine Druss.* 14(1).
- Lahaye, M., & Robic, A. (2007). Structure and functional properties of ulvan, a polysaccharide from green seaweeds. *Biomacromolecules*. 8(6), 1765–1774.
- Lindwall, G., & Cole, R. D. (1984). Phosphorylation affects the ability of tau protein to promote microtubule assembly. *Journal of Biology Chemistry*, 259(8), 5301–5305.
- Mukrasch, M. D., Biernat, J., von Bergen, M., Griesinger, C., Mandelkow, E., & Zweckstetter, M. (2005). Sites of tau important for aggregation populate {beta}structure and bind to microtubules and polyanions. *Journal of Biology Chemistry*, 280 (26), 24978–24986.
- Roberson, E. D., Scearce-Levie, K., Palop, J. J., Yan, F., Cheng, I. H., Wu, T., Gerstein, H., Yu, G., & Mucke, L. (2007). Reducing endogenous tau ameliorates amyloid β-induced deficits in an Alzheimer's disease mouse model. *Science*, 316(5825), 750–754.
- Scheltens, P., Blennow, K., Breteler, M. M. B., de Strooper, B., Frisoni, G. B., Salloway, S., & Van der Flier, W. M. (2016). Alzheimer's disease. *The Lancet*, 388(10043), 505–517.
- Senthilkumar, K., Manivasagan, P., Venkatesan, J., & Kim, S. K. (2013). Brown seaweed fucoidan: Biological activity and apoptosis, growth signaling mechanism in cancer. *International Journal of Biological Macromolecules*, 60, 366–374.
- Shi, C. J., Peng, W., Zhao, J. H., Yang, H. L., Qu, L. L., Wang, C., Kong, L., & Wang, X. B. (2020). Usnic acid derivatives as tau-aggregation and neuroinflammation inhibitors. *European Journal of Medicinal Chemistry*, 187, Article 111961.
- Smet, C., Leroy, A., Sillen, A., Wieruszeski, J. M., Landrieu, I., & Lippens, G. (2004). Accepting its random coil nature allows a partial NMR assignment of the neuronal tau protein. *Chembiochem*, 5(12), 1639–1646.
- Trinczek, B., Biernat, J., Baumann, K., Mandelkow, E. M., & Mandelkow, E. (1995).Domains of tau protein, differential phosphorylation, and dynamic instability of microtubules. *Molecular Biology of the Cell*, 6(12), 1887–1902.
- Weingarten, M. D., Lockwood, A. H., Hwo, S. Y., & Kirschner, M. W. (1975). A protein factor essential for microtubule assembly. Proceedings of the National Academy of Sciences of the United States of America, 72(5), 1858–1862.
- Wijesinghe, W. A. J. P., & Jeon, Y. J. (2012). Biological activities and potential industrial applications of fucose rich sulfated polysaccharides and fucoidans isolated from brown seaweeds: A review. *Carbohydrate Polymers*, 88(1), 13–20.
- Zhang, F., Zheng, L., Cheng, S., Peng, Y., Fu, L., Zhang, X., & Linhardt, R. J. (2019). Comparison of the interactions of different growth factors and glycosaminoglycans. *Molecules*, 24(18).
- Zhao, J., Huvent, I., Lippens, G., Eliezer, D., Zhang, A., Li, Q., Tessier, P., Robert, J. L., Zhang, F., & Wang, C. (2017). Glycan determinants of heparin-tau interaction. *Biophysical Journal*, 112(5), 921–932.
- Zhao, J., Zhu, Y., Song, X., Xiao, Y., Su, G., Liu, X., ... Wang, C. (2020). Rare 3-O-sulfation of heparan sulfate enhances tau interaction and cellular uptake. Angewandte Chemie- International Edition in English, 59(5), 1818–1827.